accordingly, using the relation between the mass center and bearing coordinates, i.e.

$$q_g=\{x,y,z,\theta_y,\theta_z\}^T,\ q_b=\{x,y_1,y_2,z_1,z_2\}^T$$

$$q_b=Tq_g,\ T=\begin{bmatrix}1&0&0&0&0\\0&1&0&0&l_1\\0&1&0&0&-l_2\\0&0&1&-l_1&0\\0&0&1&l_2&0\end{bmatrix} \quad (6)$$

The linearized equations in the bearing coordinate can be rewritten, using Eqs. (4), (5) and (6), as

$$M_b\ddot{q}_b+C_b\dot{q}_b+K_bq_b=T^{-T}K_{ig}I_m \quad (7)$$

$$I_m=\{i_1,i_2,i_3,\ldots,i_8\}^T$$

$$M_b=\begin{bmatrix}m&0&0&0&0\\0&m\bar{l}_2^2+i_d&m\bar{l}_1\bar{l}_2-i_d&0&0\\0&m\bar{l}_1\bar{l}_2-i_d&m\bar{l}_1^2+i_d&0&0\\0&0&0&m\bar{l}_2^2+i_d&m\bar{l}_1\bar{l}_2-i_d\\0&0&0&m\bar{l}_1\bar{l}_2-i_d&m\bar{l}_1^2+i_d\end{bmatrix}$$

$$C_b=\begin{bmatrix}0&0&0&0&0\\0&0&0&-\Omega i_p&\Omega i_p\\0&0&0&\Omega i_p&-\Omega i_p\\0&\Omega i_p&-\Omega i_p&0&0\\0&-\Omega i_p&\Omega i_p&0&0\end{bmatrix},$$

$$K_b=\begin{bmatrix}-K_{xx}&0&0&0&0\\0&-K_{y_1y_1}&-K_{y_1y_2}&0&0\\0&-K_{y_2y_1}&-K_{y_2y_2}&0&0\\0&0&0&-K_{z_1z_1}&-K_{z_1z_2}\\0&0&0&-K_{z_2z_1}&-K_{z_2z_2}\end{bmatrix}$$

$$K_{ig}=K_{i1}\begin{bmatrix}\beta_s&\beta_s&\beta_s&\beta_s&-\kappa\beta_s&-\kappa\beta_s&-\kappa\beta_s&-\kappa\beta_s\\\beta_c&-\beta_c&0&0&\kappa\beta_c&-\kappa\beta_c&0&0\\0&0&\beta_c&-\beta_c&0&0&\kappa\beta_c&-\kappa\beta_c\\0&0&k_1&-k_1&0&0&k_2&-k_2\\-k_1&k_1&0&0&-k_2&k_2&0&0\end{bmatrix}$$

$$K_x=4K_{q_1}(1+\eta)\beta_s,$$

$$K_{y_1y_1}=K_{z_1z_1}=K_{q_1}\left[2\beta_c^2-r_m\beta_s\beta_c\right],$$

$$K_{y_2y_2}=K_{z_2z_2}=\eta K_{q_1}\left[\beta_c^2-r_m\beta_s\beta_c\right],$$

$$K_{y_1y_2}=K_{z_1z_2}=\eta K_{q_1}r_m\beta_{2s},\ K_{y_2y_1}=K_{z_2z_1}=K_{q_1}r_m\beta_{2s},$$

$$k_1=-l_1\beta_c+R_m\beta_s,k_2=\kappa\left(l_2\beta_c-R_m\beta_s\right),$$

$$\beta_s=\sin\beta,\ \beta_c=\cos\beta,\ \eta=K_{q_2}/K_{q_1},\ \kappa=K_{i_2}/K_{i_1}$$

$$l=l_1+l_2,\ r_m=R_m/l,\ \bar{l}_1=l_1/l,\ \bar{l}_2=l_2/l,$$

$$i_d=I_d/l^2,\ i_p=I_p/l^2,\ \beta_{2s}=\sin2\beta$$

Control Algorithm

A five D.O.F. AMB system normally requires five magnet pairs for control, while only four magnet pairs is enough for control of the cone-shaped magnetic bearings. The control algorithm is constructed such that the axial displacement of the joint is controlled by

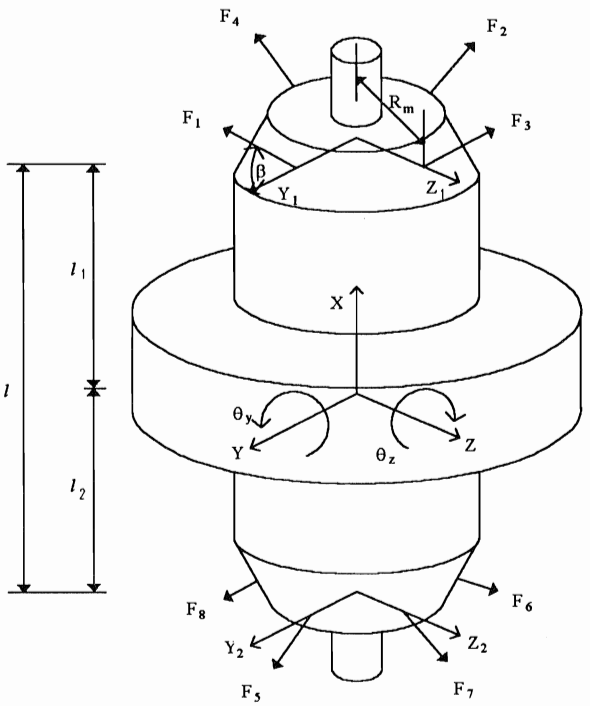

FIGURE 4 : Modeling of Cone-Shaped AMB

axial control currents to the upper and lower bearings whereas the radial displacement is controlled by radial control current to the pairs of facing radial bearings. The relation between the control current in each magnets I_m and the control current in the bearing coordinate $I_b=\{i_x,i_{y_1},i_{y_2},i_{z_1},i_{z_2}\}^T$ is written as

$$i_{1,2}=i_x\pm i_{y_1},\ i_{3,4}=i_x\pm i_{z_1},\ i_{5,6}=-i_x\pm i_{y_2},\ i_{7,8}=-i_x\pm i_{z_2} \quad (8)$$

Equations of motion in the bearing coordinate can be rewritten, using Eqs. (7) and (8), as

$$M_b\ddot{q}_b+C_b\dot{q}_b+K_bq_b=K_{ib}I_b \quad (9)$$

where

$$K_{ib}=\begin{bmatrix}K_{ixx}&0&0&0&0\\0&K_{iy_1y_1}&K_{iy_1y_2}&0&0\\0&K_{iy_2y_1}&K_{iy_2y_2}&0&0\\0&0&0&K_{iz_1z_1}&K_{iz_1z_2}\\0&0&0&K_{iz_2z_1}&K_{iz_2z_2}\end{bmatrix}$$

$$K_{ixx}=4K_{i_1}(1+\kappa)\beta_s,$$

$$K_{iy_1y_1}=K_{iz_1z_1}=2K_{i_1}\left[\beta_c-r_m\beta_s\right],$$

$$K_{iy_2y_2}=K_{iz_2z_2}=2\kappa K_{i_1}\left[\beta_c-r_m\beta_s\right],$$

$$K_{iy_1y_2}=K_{iz_1z_2}=2\kappa K_{i_1}r_m\beta_s,\ K_{iy_2y_1}=K_{iz_2z_1}=2K_{i_1}r_m\beta_s$$

For the magnetic bearing system controlled by five magnet pairs, only the diagonal terms exist in the current and displacement stiffness matrices. On the other hand, for cone-shaped AMBs, axial force induces moment because the magnetic forces exert perpendicular to the cross section area of the cone-shaped magnet. The moment couples the upper and lower

bearings, resulting in appearance of non-zero off-diagonal terms and decrease of negative diagonal terms in the displacement and current stiffness matrices. It also leads to the coupling of control inputs.

CONTROLLER DESIGN

Decoupled Controller

In Eq.(9), the axial and radial motions are decoupled, but the mass and stiffness with respect to the upper and lower bearings, and the gyroscopic coupling with respect to the y and z directional velocities take place. However, the controller may be decoupled in each direction when the gyroscopic effect due to slow rotation and the coupled terms in the stiffness matrix are negligibly small compared with the diagonal terms.

For control of the system, a simple analog type PD controller is employed, i.e.

$$V_c(s)=-K_s\left[K_p+\frac{K_d s}{\tau_d s+1}\right]Y(s) \qquad (10)$$

where K_s, K_p, K_d are the voltage gains of displacement sensor, and, the proportional and derivative control gains, respectively, and V_c is the controller output voltage.

Although the magnetic force is controlled by the current, the controller output is, in practice, the voltage. The relation between the control current in coil and the control voltage can be written as

$$V_a=Ri_c+\frac{d(Li_c)}{dt}=Ri_c+L_o\frac{di_c}{dt}+\gamma K_i\frac{dy}{dt} \qquad (11)$$

$$L\approx L_o=\frac{\mu_o N^2 A}{2g_o},\ \gamma=\frac{c}{2\alpha_g}$$

where R and L_o are the resistance and the self inductance of coil. Since the control voltages are amplified by power amplifier, self inductance of coil induces time delay that may destabilize the system. In order to reduce the time delay, the current may be incorporated with the power amplifier. In that case, Eq. (11) can be rewritten as,

$$K_a(V_o+v_c)=(K_aK_f+R)(I_o+i)+L\frac{di}{dt}+\gamma K_i\frac{dy}{dt} \qquad (12)$$

Note that I_O is determined only by the DC voltage V_o. Laplace transform of Eq. (12) yields

$$I(s)=\frac{K_c}{\tau_c s+1}V_c(s)-\frac{\gamma K_i s}{K_aK_f+R}Y(s) \qquad (13)$$

$$I_o=K_cV_o,\ \tau_c=\frac{L}{K_aK_f+R},\ K_c=\frac{K_a}{K_aK_f+R}$$

where K_a is the voltage gain of power amplifier, K_f is the current feedback gain.

The time delay between the magnetic force and the current due to the eddy current effect and flux leakage,

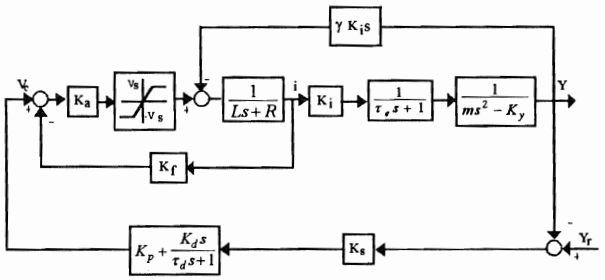

FIGURE 5 : Block Diagram of 1 D.O.F. System

may be incorporated as [6].

$$F(s)=\frac{K_i}{\tau_e s+1}I(s) \qquad (14)$$

where τ_e is the time constant associated with the eddy current effect.

Stability Analysis

When the bearing is assumed to be a first order device, **FIGURE** 5 shows the corresponding block diagram. The closed-loop transfer function can be written as

$$\frac{Y}{Y_r}=\frac{k_p+k_r s}{as^4+bs^3+cs^2+ds+e} \qquad (15)$$

where

$$a=\tau_c\tau_d, b=(\tau_c+\tau_d)m, c=m, d=(k_r-\tau_d K_y), e=(k_p-K_y)$$

$$k_p=K_sK_cK_iK_p, k_r=K_sK_cK_iK_r, K_r=K_d+\tau_d K_p$$

The stable control gain resigns for the magnetic bearing system (15) can be obtained, by using the Routh-Hurwitz stability criteria, as

$$\tau_d K_{pl}<K_r<\tau_d K_{pl}+\frac{(\tau_d+\tau_c)m}{K_sK_cK_i\tau_d\tau_c} \qquad (16)$$

$$K_{pl}<K_p<K_{pl}+\frac{(K_r-\tau_d K_{pl})}{(\tau_d+\tau_c)}-\frac{\tau_d\tau_c K_sK_cK_i}{m(\tau_d+\tau_c)^2}(K_r-\tau_d K_{pl})^2$$

$$K_{pl}=\frac{K_y}{K_sK_cK_i}$$

Using the above equation and the relation $K_d=K_r-\tau_d K_p$, we can find K_p and K_d so that the system is stable. The minimum and maximum values of K_p are determined once K_{pl} and K_d are selected. **TABLEs** 1 and 2 show the system parameters and the poles. The time delays are: τ_d=8×10^{-5}sec and τ_c=6×10^{-5}sec so that 4.8×10^{-5}sec<K_r<0.0175sec and the minimum value of K_p becomes 0.6. For K_r = 0.005, the maximum value of K_p is 34.9. **FIGUREs** 6(a) and 6(b) are the stable start-up and impulse responses. The system stiffness increases as the proportional gain increases. However, as shown in **FIGURE** 6, unstable response occurs due to saturation of the supply voltage and flux density, and due to magnetic force nonlineari-

TABLE 1 System Parameters

Parameter	Value
Pole face area, A	155 mm^2
Inclined angle, β	15°
Nominal gap, g_o	0.5 mm
Rotor mass, m	1.68 kg
Coil turns, N	400/magnet
Power supply voltage, V_s	25 Volt
Force in radial dir.	117N/magnet
Force in axial dir.	27N/magnet
System size	H130mm×ϕ130mm

TABLE 2 Eigenvalues of AMBs System

	Uncontrolled	Controlled
Eigenvalues	±249.5	-236.7±j320.7
	±341.6	-368.1±j480.4
	±382.8	-454.8±456.7

ty. As the derivative gain increases, the system damping also increases, but it tends to amplify high frequency noise. The control gains are determined such that the system has the damping ratio of 0.5 and the stiffness of 1.5×10^5N/m.

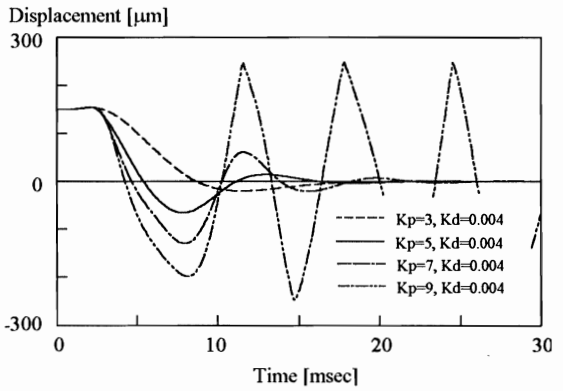

(a) Start-up Response

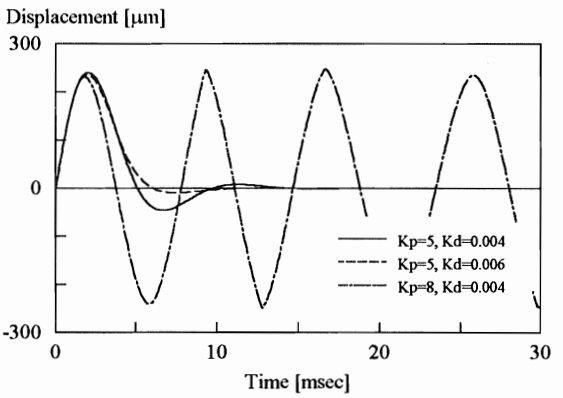

(b) Impulse Response

FIGURE 6 : Time Response (simulation)

EXPERIMENT

The maximum moment M_{max} is an important factor to be considered in the design of a robot joint, which can be expressed as

$$M_{max}=\frac{AB_{max}^2D}{\mu_o}[\tan\beta-\tan\alpha] \qquad (17)$$

where B_{max} is the saturation magnetic flux density of core material, $\tan\alpha=l/D$, l is the height of two magnetic bearings and $D=2R_m$ is the effective diameter of rotor core. Since B_{max} normally takes the value of 1.0 Tesla and the robot joint shape(α) is given, the remained design parameters are the cross-section area(A) and the inclined angle(β) of core. When the cross-section area(A) is chosen in consideration of maximum magnetic force, the inclined angle(β) of core is determined to be 15° such that the maximum moment is 8 N-m per magnet.

FIGURE 7 shows the stable start-up response for the initial condition q_b={-297.8, -126, -147.5, 129.7, -89.3}$^T\mu m$. The low supply voltage produces the large time delay and settling time, and the time delay is mainly associated with raising the current to nominal bias values. Response to axial impact is shown in **FIGURE** 8. The natural frequency and damping ratio estimated from the impact test are found to be 64.1Hz and 0.476, which are in good agreement with the analytical results of 63.4Hz and 0.59.

CONCLUSION

A magnetically suspended robot joint is developed, which is free of dust and oil generation. Two radial bearings consisting of cone-shaped magnet cores control the rotor motion in the axial and radial directions. A linearized dynamic model is developed for active control of the magnetic bearing system. The control algorithm is constructed such that the axial displacement of the joint is controlled by axial control currents to the upper and lower bearings whereas the radial displacement is controlled by radial control current to the pairs of facing radial bearings. The stability and control performance is tested through numerical simulation based on the nonlinear model. Experiments are performed to investigate the dynamic characteristics of the system. Comparison between the experimental and simulation results shows that modal parameters estimated from analysis and experiments agree well within the error less than 10% and that the motion of the magnetically suspended robot joint can be well predicted by the analytical work.

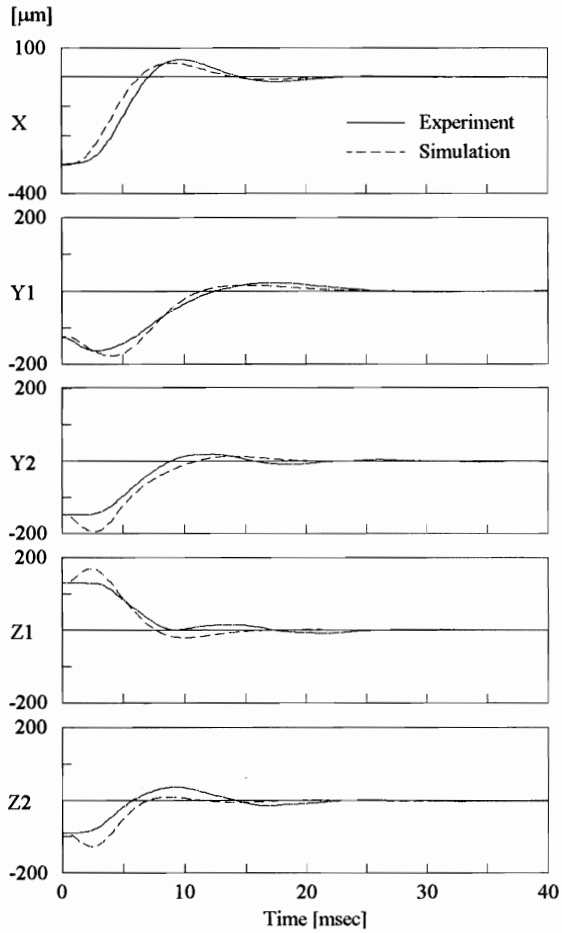

FIGURE 7 : Start-up Response (experiment)

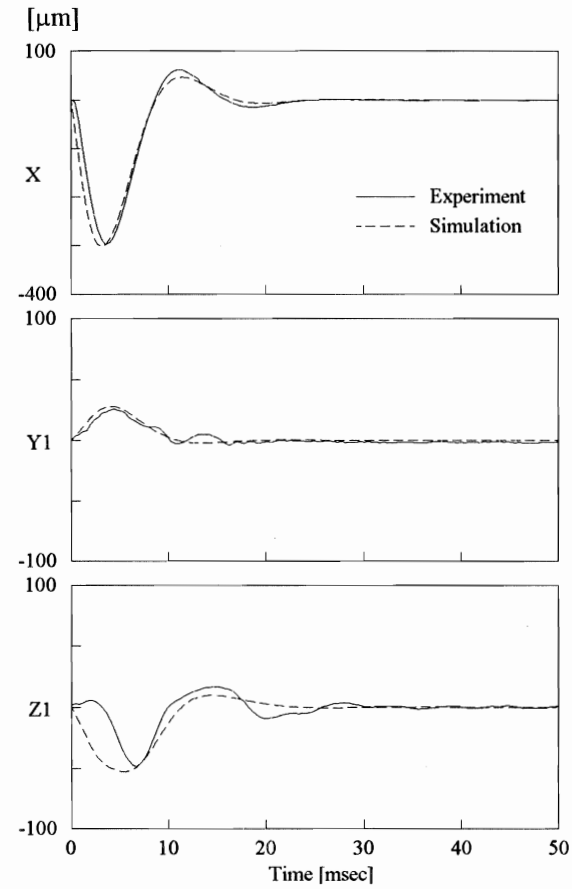

FIGURE 8 : Impulse Response (experiment)

REFERENCES

1. Dussaux, M., "The Industrial Applications of the Active Magnetic Bearings Technology," *Proc. of the 2nd Int'l Symp. on Magnetic Bearings*, Tokyo, pp33-38, 1990.
2. Kim, J. S., Lee, C. W., "Modal Testing and Suboptimal Vibration Control of Flexible Rotor Bearing System using a Magnetic Bearing," *Trans. ASME Journal of Dynamic System Measurement and Control*, Vol. 114, June, pp244-252, 1992.
3. Lee, C. W., Kim, C. S., "Isotropic Control of Rotor Bearing System," *Proc. of 14-th ASME conference on Mechanical Vibration and Noise*, Albuquerque, pp325-330, 1993.
4. Higuchi, T., Oka, K. and Sugawara, H., "Development of Clean Room Robot with Contactless Joints using Magnetic Bearing," *Proc. of USA-Japan Symp. on Flexible Automation*, Vol. 1, pp229-243, 1988.
5. Fukata, S., "Linearized Model and Control System of Active Magnetic Bearings with Magnet Cores in the Shape of a Cone," *JSME Series (C)*, Vol.58, No. 551, pp75-82, 1992(in Japanese).
6. Zmood, R. B., Anand, D. K., Kirk, J. A., "The Influence of Eddy Currents on Magnetic Actuator Performance," *Proc. of IEEE* Vol. 75, No. 2, pp259 -260, 1987.